Electrostatic Influences on the Kinetics of the Reactions of Lobster Metallothioneins with the Electrophilic Disulfides 2,2′-Dithiodipyridine (PySSPy) and 5,5′-Dithiobis(2-nitrobenzoic acid) (ESSE)

Zhiwu Zhu, David H. Petering, and C. Frank Shaw III*

Department of Chemistry and the UWM-NIEHS Aquatic and Marine Biomedical Core Center, University of Wisconsin—Milwaukee, P.O. Box 413, Milwaukee, Wisconsin 53201-0413

Received March 8, 1995[⊗]

Metallothioneins (MT) are ubiquitous proteins which can interact with electrophiles including alkylating agents and gold- and platinum-dependent chemotherapeutic agents and reactive oxygen species. Crustacean MTs are useful model systems due to modifications of stoichiometry and structure. Electrostatic influences on the reactions of lobster hepatopancreas MT-1 and MT-2 with two electrophilic disulfides were investigated. 5,5′-Dithiobis-(2-nitrobenzoic acid), ESSE, and 2,2′-dithiodipyridine, PySSPy, react biphasically. Each phase has disulfide dependent and independent terms, yielding a four-term rate law: rate = k_{1s}[MT] + k_{2s}[RSSR][MT] + k_{1f}[MT] + k_{2f}[RSSR][MT]. The neutral disulfide PySSPy reacts more rapidly and has significantly greater second order rate constants than the negatively (−2) charged DTNB. The MT-1 rate constants in 5 mM Tris-HCl-100 mM KCl buffer, pH 7.4, at 25 °C are k_{2f} = 52.5 and k_{2s} = 3.65 M^{-1} s^{-1} for PySSPy and k_{2f} = 5.80 and k_{2s} = 0.70 M^{-1} s^{-1} for ESSE. Ionic strength studies of the reactions of ESSE and MT-1 showed a positive salt effect with increasing KCl concentration, as expected for a reaction between similarly charged species. The Debye–Huckel law, applied to k_{2f} and k_{2s}, yielded effective charges of −1 for the two protein reaction centers. These values agree with the charges of the two domains (β_C and β_N) and support a kinetic model in which each phase of the reaction is associated with one of the domains. The reactivities are discussed in light of the novel cadmium–thiolate connectivities of the lobster MT domains.

Introduction

Metallothioneins (MT),[1-5] a class of proteins typically having about 60 amino acids, including 18–20 cysteines, and binding 6–12 heavy metal ions, are the subject of intense efforts to elucidate their chemical and physiological properties. Cd(II) induction of metallothionein[3] suggests that MT may be involved in the detoxification of this toxic ion. Additional evidence suggests that metallothionein may play a role in the metabolism of zinc and copper.[1-4] Other putative functions include postulated roles for the cysteine ligands in reactions with organic and heavy-metal electrophiles and oxidants.[5] The details of the MT structure revealed by ^{113}Cd-NMR,[6] 2D-NMR,[7,8] X-ray,[9] and chemical methods[10] have enhanced our understanding of this unique protein. Mammalian metallothioneins contain two metal clusters located in distinct domains: M_4S_{11} and M_3S_9 (M = Cd(II) or Zn(II), S = cysteinyl thiolate) in the α (C terminal) and β (N-terminal) domains, respectively. Each metal ion is tetrahedrally coordinated by terminal and bridging thiolates.

The cysteine residues, in addition to chelating various heavy metal ions, provide a source of nucleophilic sulfhydryl groups.[5,11-18] They have been highly conserved through the long history of mammalian evolution but are conserved differently among crustacean species. The conservation of the MT cysteines suggests that their functional importance exceeds the mere ability to coordinate promiscuously to heavy metal ions. Thus, exploring their kinetic reactivity is a key approach to understanding the putative functions of metallothionein.[2,11] Among the various electrophiles examined, 5,5′-dithiobis(2-nitrobenzoic acid) (ESSE or DTNB), which reacts directly with the cysteine thiolates, has been most studied.[10,12-15] Recently, Savas *et al.*[17] and Maret[18] independently reported that oxidized glutathione (GSSG), a disulfide reagent with a net −2 charge, reacts with MT releasing the coordinated metal ions. While the biological significance remains uncertain due to the low concentrations of GSSG in cells, interest in the mechanism of this reaction is a stimulus to further kinetic studies with analogous disulfides.

[⊗] Abstract published in *Advance ACS Abstracts,* July 15, 1995.

(1) Kägi, J. H. R.; Kojima, Y. *Metallothionein II*; Birkhäuser Verlag: Basel, 1987.
(2) Stillman, M. J.; Shaw, C. F., III; Suzuki, K. T. *Metallothioneins*, VCH: New York, 1992.
(3) Hamer, D. *Annu. Rev. Biochem.* **1989**, *55*, 913–952.
(4) Richards, M. P. *J. Nutr.* **1989**, *119*, 1062.
(5) Karin, M. *Cell* **1985**, *41*, 9–10.
(6) Otvos, J. D.; Armitage, I. M. *Proc. Natl. Acad. Sci. U.S.A.* **1980**, *77*, 7094–7098.
(7) Frey, M. H.; Wagner, G.; Vasâk, M.; Sorensen, O. W.; Neuhaus, D.; Worgotter, E.; Kägi, J. H. R.; Ernest, R. R.; Wutrich, K. *J. Am. Chem. Soc.* **1985**, *107*, 6847–6851.
(8) Arseniev, A.; Schultze, P.; Worgotter, E.; Brown, W.; Wagner, G.; Vasâk, M.; Kägi, J. H. R.; Wutrich, K. *J. Mol. Biol.* **1988**, *201*, 637–657
(9) Robbins, A. H.; McRee, D. E.; Williamson, M.; Collett, S. A.; Xuong, N. J.; Furey, W. F.; Wang, B. C.; Stout, C. D. *J. Mol. Biol.* **1991**, *221*, 1269.
(10) Winge, D. R.; Miklossy, K.-A. *J. Biol. Chem.* **1982**, *257*, 3471–3476.
(11) Otvos, J. D.; Petering, D. H.; Shaw, C. F., III. *Comments Inorg. Chen.* **1990**, *9*, 1–35.
(12) Li, Ti-Y.; Minkel, D. T.; Shaw, C. F., III; Petering, D. H. *Biochem. J.* **1981**, *193*, 441–446.
(13) Shaw, C. F., III; Laib, J. E.; Savas, M. M.; Petering, D. H. *Inorg. Chem.* **1990**, *29*, 4k03–408.
(14) Savas, M. M.; Petering, D. H.; Shaw, C. F., III. *Inorg. Chem.* **1991**, *30*, 581–583.
(15) Bernhard, W. R.; Vasâk, M.; Kägi, J. H. R. *Biochemistry* **1986**, *25*, 1975–1980.
(16) Zhu, Z.; Goodrich, M.; Isab, A. A.; Shaw, C. F., III. *Inorg. Chem.* **1992**, *31*, 1662–1667.
(17) Savas, M. M.; Petering, D. H.; Shaw, C. F., III. *J. Inorg. Biochem.* **1993**, *52*, 235–249.
(18) Maret, W. *Proc. Natl. Acad. Sci. U.S.A.* **1994**, *91*, 237–241.

0020-1669/95/1334-4477$09.00/0

The two domains of MT react independently with ESSE, giving rise to biphasic reactions.[12,14,15] The isolated α-domain exhibits monophasic kinetics characteristic of the faster reaction phase,[14] while the β domain reacts monophasically and slowly (Munoz, A.; Petering, D. H.; Shaw, C. F., III. Unpublished work). These results conclusively eliminate the bridging and terminal thiolates as the source of the biphasic kinetics but do not distinguish whether the two unique metal clusters (M_4S_{11} and M_3S_9) or the α- and β-domains that respectively enfold them cause the differential reactivity. Crustacean MTs contain 18 cysteines, which form two three-metal clusters.[19-23] Our recent 2-D NMR studies of the lobster MT-1 establish unequivocally that the two clusters are located in distinct domains. They are designated β_c and β_n since each contains a type B or three-metal cluster.[22,23]

The recently reported biphasic reaction of ESSE and lobster MT-2,[16] if it is a general property, has important implications for the origin of the biphasic reactions of mammalian MTs.[12,14,15] Therefore, we investigated and report here the reactions of ESSE with lobster Cd_6MT-1 and of the related aromatic disulfide, 2,2′-dithiodipyridine (PySSPy) with both lobster isoproteins. PySSPy ($pK_1 < 1$ and $pK_2 = 2.45$)[24] is a neutral species under physiological conditions (as confirmed by NMR titrations in the present study) and therefore useful for probing structure function relationships, especially the role of electrostatic influences, in MT−disulfide reactions.

Experimental Section

Materials. Sephadex G-75, G-25, and G-10, DEAE Sephadex A-25-120, Trizma base and β-mercaptoethanol were purchased from Sigma Biochemicals; (phenylmethyl)sulfonyl fluoride (PMSF) and 5,5′-dithiobis(2-nitrobenzoic acid) (ESSE) from Aldrich Chemical Co., Inc.; 2,2′-dipyridyl disulfide (PySSPy) from Lancaster Synthesis. PySSPy stock solution was prepared by following the method described elsewhere[25] and its concentration was determined spectrophotometrically by using $\epsilon_{281} = 9730\ M^{-1}\ cm^{-1}$.[26]

Isolation of Lobster MTs. The procedures for lobster husbandry and isolation of *lob*-Cd_6MTs were described previously.[16,23] The lobster MT band isolated after Sephadex G-75 chromatography was applied to a DEAE column and eluted with a gradient of 20−300 mM Tris−HCl buffer + 2 mM β-mercaptoethanol, pH 7.4, then desalted over Sephadex G-15. The MT-1, -2, and -3 isoforms were well separated. When traces of copper were present they were removed by acidification in 1 M HCl for 30 min, followed by elution over Sephadex G-25 in 50 mM HCl and neutralization to pH 7.4 with solid Tris base in the presence of mercaptoethanol and a slight excess of Cd^{+2} (6.5 equiv). After concentration in using an Amicon YM-2 membrane, the final purification was over Sephadex G-50 (2.5 × 105 cm) column at flow rate of 1 drop/s. The MT-1 and MT-2 isoproteins, after carboxymethylation, showed only a single band by SDS-PAGE electrophoresis. Each isoform was examined by ^{111}Cd NMR and exhibited the expected six resonances. Further verification of protein integrity was obtained by measuring the S^-/Cd ratios determined using PySSPy (Cd_6MT-1, 2.99 ± 0.11, and Cd_6MT-2, 3.01 ± 0.10; theoretical 3.0). An amino acid analysis has been previously reported for MT-2.[16] Both isoforms exhibit a 250 nm UV shoulder, characteristic of Cd−S charge transfer interactions.

Table 1. [ESSE] and pH Dependence of the Observed Rate Constants for the Reaction of Lobster Cd_6MT-1 with ESSE[a]

[ESSE]/mM	pH	$(k_s \pm \sigma) \times 10^3/s^{-1}$	$(k_f \pm \sigma) \times 10^2/s^{-1}$
0.5	7.4	1.20 ± 0.06	0.65 ± 0.10
1.0	7.4	1.87 ± 0.11	1.12 ± 0.02
2.0	4.7	2.89 ± 0.02	1.81 ± 0.05
2.0	6.0	2.89 ± 0.07	1.99 ± 0.04
2.0	6.8	2.94 ± 0.04	1.92 ± 0.06
2.0	7.4	2.64 ± 0.58	1.68 ± 0.01
2.0	8.1	2.75 ± 0.06	1.94 ± 0.06
3.0	7.4	3.39 ± 0.08	2.31 ± 0.06
4.0	7.4	3.92 ± 0.11	2.75 ± 0.03
5.0	7.4	4.43 ± 0.18	3.34 ± 0.06

[a] $[Cd]_{MT} = 20\ \mu M$; in 5 mM Tris−HCl + 100 mM KCl at 25 °C.

Kinetics. The conditions for monitoring the reactions of *lob*-Cd_6-MT-1 with ESSE were the same as those for *lob*-Cd_6-MT-2 in our previous studies.[10] The reactions were followed with a Perkin-Elmer Lambda 6 UV/Vis spectrophotometer equipped with a circulating water bath set at 25.0 ± 0.1°. The ionic strength dependence of the rate constants for the reaction of *lob*-Cd_6MT-1 with ESSE was examined by varying the KCl concentrations: 25, 50, 100, 200, and 400 mM. The data were fitted by the extended Debye−Hückel relationship.

The reactions of Cd_6MT-1 and Cd_6MT-2 with PySSPy were set up under pseudo-first-order conditions ([PySSPy] ≫ [MT thiolate]) in 5 mM Tris−HCl buffer of pH 7.4 and followed at 343 nm over time against a reference containing an equivalent amount of PySSPy. Cd_6-MT-1 and Cd_6MT-2 were measured as Cd and kept constant at 5 μM. The PySSPy concentration, limited by its solubility, was varied from 0.2 to 0.8 mM. The pH dependence of the rate constants for the reaction of Cd_6MT-2 with PySSPy was determined using 0.2 mM DTP at different pHs: 5.0, 5.7, 6.3, 7.0, 7.4, and 8.3.

Absorbance vs time data from the UV spectrophotometer were transferred to Quattro Pro and analyzed using standard algorithms for biphasic reactions,[27] as described elsewhere.[12,16]

Results

Kinetics of Reaction of *lob*-Cd_6MT-1 with ESSE. In order to compare the reactivity of the lobster MT-1 and MT-2 isoforms, the reactions of Cd_6MT-1 were performed under the same pseudo-first-order conditions ([ESSE] ≫ [MT]) used previously with Cd_6MT-2.[16] The reaction generates 18 equiv of thionitrobenzoate (ES^-), indicating that it goes to completion. The absorbance changes plotted as $\ln(A_\infty - A_t)$ vs time exhibit biphasic kinetics. Two observed rate constants (k_f and k_s) were calculated according to the standard kinetic treatment for parallel reactions.[27] The ESSE concentration dependence of the observed rate constants is demonstrated by the data in the Table 1. These rate constants are 5- to 8-fold faster than those for the corresponding mammalian MTs under the same conditions and comparable to those for Cd_6MT-2. Figure 1 shows the linear relationship between the observed rate constants and ESSE concentration. The finite intercepts for the plots of k_f and k_s indicate that each phase of the reaction consists of ESSE dependent and independent terms. Thus, the reaction is described by the following four-term rate law:

$$\text{rate} = k_{1s}[MT] + k_{2s}[ESSE][MT] + k_{1f}[MT] + k_{2f}[ESSE][MT] \quad (1)$$

The values of the four rate constants are given in Table 5 and will be considered in the Discussion.

The pH dependence of the observed rate constants was examined from pH 4.7 to 8.1 with [ESSE] fixed at 2 mM. Table 1 shows that varying the pH did not influence the rate constants. This result is consistent with the pK_a values of ESSE and the

(19) Brouwer, M., Winge, D. R., Gray, W. R. *J. Inorg. Biochem.* **1989**, *35*, 289−303.
(20) Otvos, J. D.; Olafson, R. W.; Armitage, I. M. *J. Biol. Chem.* **1982**, *257*, 2427−2431.
(21) Lerch, K.; Ammer, D.; Olafson, R. W. *J. Biol. Chem.* **1982**, *257*, 2420−2426.
(22) Zhu, Z. Ph.D. Thesis, University of Wisconsin−Milwaukee, 1993.
(23) Zhu, Z.; DeRose, E.; Petering, D.; Shaw, C. F., III. *Biochemistry* **1994**, *33*, 8858−8865.
(24) Brocklehurst, K.; Little, G. *Biochem. J.* **1973**, *133*, 67−80.
(25) Jocelyn, P. C. *Methods Enzymol.* **1987**, *143*, 44−67.
(26) Griffith, D. R.; Murray, J. F., Jr. *Arch. Biochem. Biophys.* **1967**, *119*, 41−49.
(27) Espenson, J. H. *Chemical Kinetics and Reaction Mechanism*, McGraw-Hill: New York, 1981; pp 55−56.

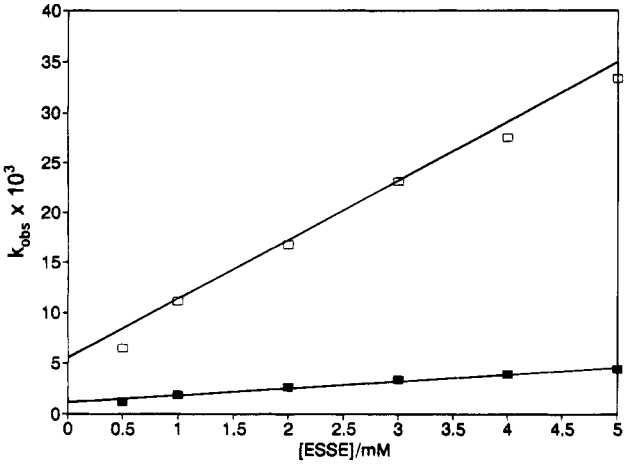

Figure 1. Plots of the observed rate constants vs [ESSE] for reactions of lobster Cd_6MT-1. k_s (■), k_f (□). Conditions: [ESSE] = 0.5−5.0 mM, $[Cd]_{MT}$ = 20 μM, and pH 7.4 in 5 mM Tris−HCl buffer with 100 mM KCl at 25 °C.

amino acid side chains of metallothionein, since neither molecule has any functional groups that can be protonated or deprotonated in this pH range.

^{1}H NMR pH Titration of PySSPy. 2,2′-Dithiopyridine (PySSPy) is an aromatic disulfide which generates a UV chromophore upon reaction with thiols:

$$\text{PySSPy} + \text{RSH} \rightarrow \text{RSSPy} + \text{Py=S} \qquad (2)$$

The kinetics and extent of reaction can be monitored using the absorbance change at 343 nm. Thus, PySSPy is an attractive probe molecule for structure-function studies on MT. The extent to which PySSPy is protonated to form mono- or dications must be known confidently to interpret the kinetic data, but examination of the literature revealed surprisingy low pK_a values for $PySSPyH_2^{2+}$ ($pK_1 < 1$ and $pK_2 = 2.45$).[24] Therefore, to test the literature pK_a values, ^{1}H NMR titrations of PySSPy were performed. The resonances of protons H-3, H-4, H-5, and H-6 of the pyridine ring are sensitive to electronic changes upon protonation of the nitrogen atom. The starting pH of the titration was high to assure that a very large pK_a value had not been overlooked in previous UV spectral titrations.[24] The results (Figure 2) confirm the absence of any protonation between pH 9.2 and 3.5. Below pH 3.5, significant changes are observed, consistent with the literature value $pK_2 = 2.45$.

Kinetics of Reaction of Cd_6MT-2 with PySSPy. PySSPy (confirmed to be neutral at pH 7.4) was used for structure function studies on the reactivity of lobster MT thiolates. Reactions of Cd_6MT-2 with a pseudo-first-order excess of PySSPy were monitored at 343 nm and went to completion within 5−25 minutes depending on pH and [PySSPy]. From the final absorbance values and the extinction coefficient of Py=S, the reaction was determined to go to completion at all PySSPy concentrations studied. The average value of $[RS^-]/[Cd]$, 2.9 ± 0.2, is experimentally equal to the ratio of 3.0 calculated from the composition of lobster MT-2. Thus, the following stoichiometry is obtained:

$$\text{excess PySSPy} + Cd_6MT \rightarrow \text{oxidized MT} + 6Cd^{+2} + 18\text{Py=S} \qquad (3)$$

Plotting $\ln(A_\infty - A_t)$ vs time revealed that the reactions are biphasic. Figure 5 shows a typical plot obtained with 0.3 mM PySSPy. The magnitudes of the observed rate constants for the fast and slow steps, calculated according to standard kinetic treatments,[27] show that the PySSPy reactions are faster (Table 2) than those of ESSE at comparable concentrations.[16] The PySSPy concentration dependence was studied. The resulting slow and fast step observed rate constants (Table 2), when plotted against [PySSPy], exhibit finite intercepts and linear relationships over the entire concentration range studied 0.3−0.8 mM (Figure 6). Thus, a four-term rate law is obtained:

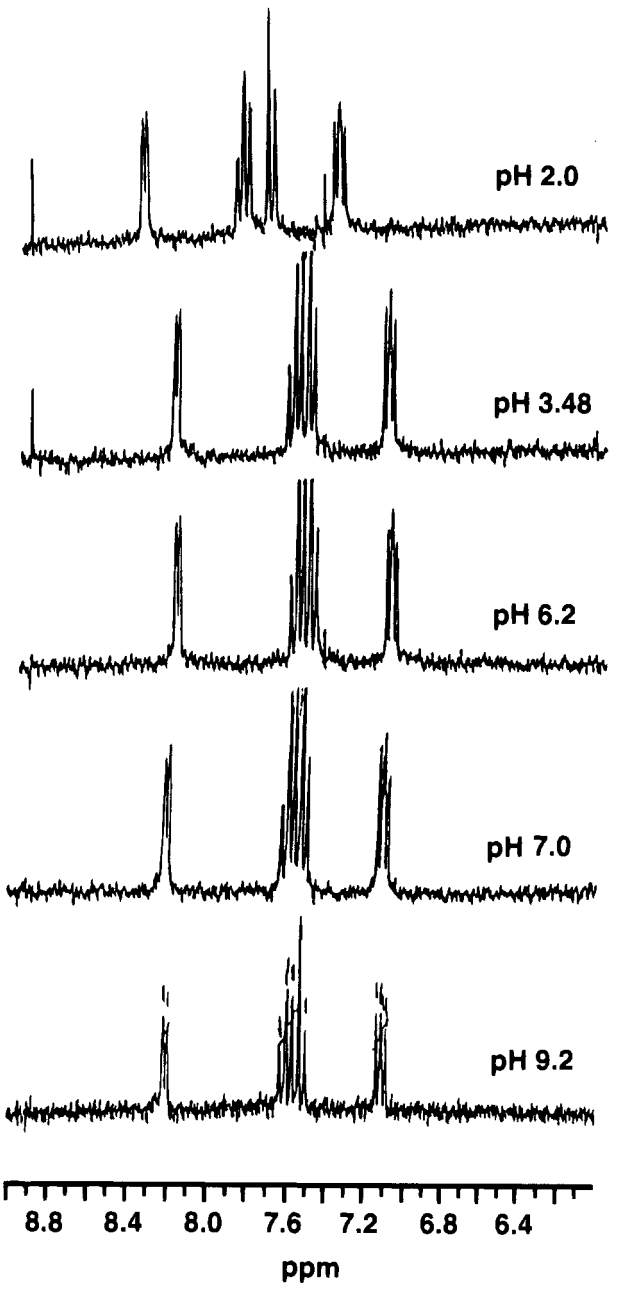

Figure 2. ^{1}H NMR pH (500 MHz) titration of PySSPy (900 μM) in 99.96% D_2O. The pH was initially adjusted to pH 9.2 with NaOD, and then decreased by sequential additions of conc. DCl.

$$\text{rate} = k_{1s}[\text{MT}] + k_{2s}[\text{PySSPy}][\text{MT}] + k_{1f}[\text{MT}] + k_{2f}[\text{PySSPy}][\text{MT}] \qquad (4)$$

This expression is similar to that for ESSE reactions, eq 1. Because the rate constants and form of the expression are determined by stepwise analysis of the data (fast and slow observed rate constants for each PySSPy concentration are plotted against [PySSPy] to yield the four components), the contribution of each term is more certain than would be the case if a single kinetic run were fit to four terms by a curve fitting procedure. The magnitudes of the first-order rate constants are close to those of ESSE reaction, but the second-

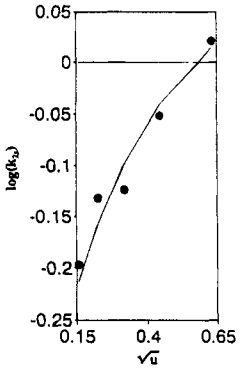

Figure 3. Plots of $\ln(k_{2s})$ vs μ for the reaction of lobster Cd_6MT-1 with ESSE. Conditions: $[Cd]_{MT} = 20\ \mu M$, at 25.0 °C, in 5 mM Tris–HCl buffer with [KCl] = 25, 50, 100, 200, and 400 mM. At each [KCl] reactions were run with [ESSE] = 1.0, 2.0, 3.0, 4.0, and 5.0 mM, then the actual second-order rate constants were determined from the fast and slow observed rate constants.

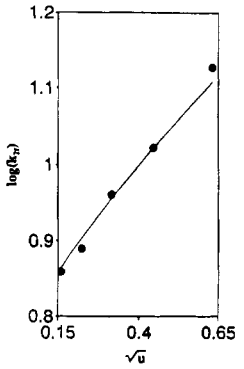

Figure 4. Plots of $\ln(k_{2f})$ vs μ for the reaction of lobster Cd_6MT-1 with ESSE. Conditions are the same as in Figure 3.

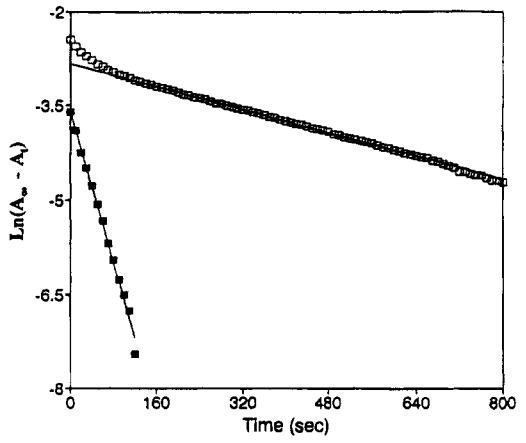

Figure 5. Biphasic reaction profile for the PySSPy with lobster Cd_6-MT-2: (□) $\ln(A_\infty - A_t)$; (■) $\ln[(A_\infty - A_t)_{tot} - (A_\infty - A_t)_{slow}]$, which represents the fast step after subtracting out the slow step.[27] Conditions: [PySSPy] = 0.3 mM, $[Cd]_{MT} = 20\ \mu M$, and pH 7.4 in 5 mM Tris–HCl buffer with 100 mM KCl at 25.0 °C.

order rate constants are much greater (Table 5) and will be discussed below.

pH Dependence of the Reaction of Cd_6MT-2 with PySSPy. The pH dependence of the reaction was examined over the range 5.0 to 8.3 with the PySSPy concentration held constant. The range is limited by the dissociation of Cd^{+2} below pH 5 and by hydroxide-induced cleavage of PySSPy at higher pH values. Although no pH dependence was expected, since neither PySSPy nor MT have groups protonatable in this range, a systematic increase in the reaction with increasing H^+ (decreasing pH) was observed (Table 2). The rate constant for the fast step, k_f, increases 10-fold, and k_s increases more than 3-fold.

Table 2. [PySSPy] and pH Dependence of the Observed Rate Constants for the Reaction of Lobster Cd_6MT-2[a]

pH	[PySSPy]/mM	$(k_s \pm \sigma) \times 10^3/s^{-1}$	$(k_f \pm \sigma) \times 10^2/s^{-1}$
5.0	0.2	2.67 ± 0.02	4.04 ± 0.22
5.7	0.2	2.71 ± 0.08	3.62 ± 0.25
6.3	0.2	1.80 ± 0.14	2.27 ± 0.34
7.0	0.2	1.19 ± 0.09	1.61 ± 0.07
7.4	0.2	1.02 ± 0.05	1.37 ± 0.02
7.4	0.3	2.17 ± 0.10	3.45 ± 0.10
7.4	0.4	2.96 ± 0.11	4.22 ± 0.14
7.4	0.5	3.72 ± 0.15	5.38 ± 0.18
7.4	0.6	4.36 ± 0.07	6.32 ± 0.20
7.4	0.8	5.01 ± 0.76	8.62 ± 0.65
8.3	0.2	0.75 ± 0.02	0.36 ± 0.00

[a] $[Cd]_{MT} = 5\ \mu M$; 5 mM Tris–HCl + 100 mM KCl at 25.0 °C.

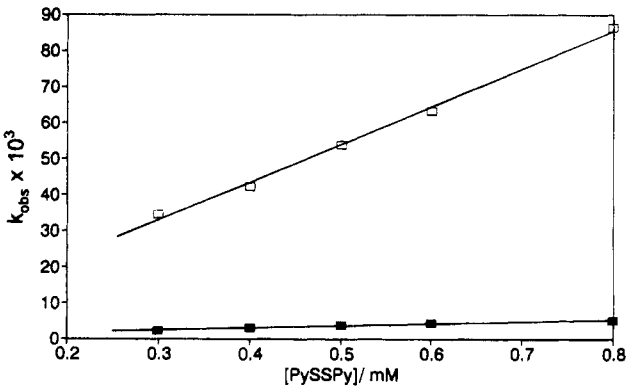

Figure 6. Plots of the observed rate constants vs [PySSPy] for the reaction of Cd_6MT-2 with PySSPy: k_s (■); k_f (□). Conditions: $[Cd]_{MT} = 5\ \mu M$, pH 7.4 in 5 mM Tris–HCl buffer with 100 mM KCl at 25.0 °C, and [PySSPy] = 0.2–0.8 mM.

The rates of the ESSE reactions described are pH independent in this range. Thus, participation of the proton in the disulfide bond cleavage step, which is common to both PySSPy and ESSE, is not a feasible explanation of the pH dependence. The low pK_a values of PySSPy (confirmed by the titration of Figure 2) are inconsistent with an effect due to the protonation of the pyridine rings of PySSPy. Quantitative argument support this view. If a small amount of $PySSPyH^+$ were formed and were extremely reactive, the fast and/or slow step observed rate constants should include terms for the cation:

$$k_{obs} = k_+[PySSPyH^+] + k_o[PySSPy] \quad (5)$$

The concentration of $[PySSPyH^+]$ in terms of C_{PySSPy}, the total PySSPy present, is given by $[H^+]C_{PySSPy}/([H^+] + K_2)$, where $K_2 = 10^{-2.15}$. In the pH range 5–8, $[H^+] \ll K_2$ with the consequence that $[PySSPyH^+] \ll [PySSPy]$ and therefore that $[PySSPy] \approx C_{PySSPy}$. Substitution yields $[PySSPyH^+] = [H^+][PySSPy]/K_2$, which can be further substituted into eq 5 to generate eq 6. Equation 6 predicts a linear dependence on $[H^+]$,

$$k_{obs} = \{(k_+/K_2)[H^+] + k_o\}[PySSPy] \quad (6)$$

but in contrast, plots of k_f and k_s vs $[H^+]$ (not shown) exhibit saturation behavior, ruling out reaction of $PySSPyH^+$ as the explanation of the pH dependence.

Alternatively, the pyridine rings of PySSPy are potential metal ligands. Coordination of PySSPy to a cluster Cd^{+2} with concomitant displacement of a cysteine thiolate would subject the latter to protonation:

$$\text{protein}{-}Cd_3SCy_9 + PySSPy + H^+ \rightleftharpoons HSCy{-}\text{protein}{-}Cd_3SCy_8(PySSPy) \quad (7)$$

While acid-dissociation of Cd^{+2} from lobster MT-2 occurs only at pH values below 5,[16] the additional driving force of a ligand exchange equilibrium involving PySSPy should shift the protonation toward neutral pH values, as observed. Brouwer et al. have proposed a competition analogous to eq 7 in which glutathione binds to the homologous blue crab MT and displaces a Cd-bound cysteine residue.[28] According to eq 7, acidic conditions favor the thiol displacement by PySSPy, which, in turn, allows the liberated thiol to react with additional PySSPy more rapidly than as a cadmium-bound thiolate, as observed.

Kinetics of Reaction of Cd_6MT-1 with PySSPy. Reactions of Cd_6MT-1 with PySSPy were carried out under the same conditions as those of Cd_6MT-2, above. The observed rate constants show linear relationships with [PySSPy] over a range from 0.3 mM to 0.9 mM (Table 3 and Figure 7). Thus this reaction also obeys the four-term rate law of eq 4. The first- and second-order rate constants are listed in Table 5 and considered further in the Discussion.

Ionic Strength Dependence of the Reaction of Cd_6MT-1 with ESSE. The accelerated reactions of PySSPy suggest that the negative charge of ESSE may affect its rate of reaction with MT since both are negatively charged. Therefore, the ionic strength dependence of the reaction between Cd_6MT-1 and ESSE was investigated. At five different concentration of NaCl, with pH held constant at 7.4 and temperature at 25.0 ± 0.1°, the reaction rates were measured as a function of [ESSE] in order to calculate the four rate constants which fully describe the reaction kinetics. The ionic strength dependence of the first- and second-order rate constants is shown in Table 4. The second-order rate constants (k_{2s} and k_{2f}) increase with ionic strength, a behavior characteristic of reactions between identically charged species. Thus, the positive ionic strength effects on the rate constants k_{2s} and k_{2f} demonstrate significant electrostatic contributions to the activation energy for each second order step.

The extended Debye Hückel relationship,[29] which is nonlinear due to the two-term denominator, was applied to determine the effective charges on the reaction centers associated with each second-order reaction component:

$$\log k = \log k_o + \frac{2AZ_iZ_j\sqrt{u}}{1 + Br_2\sqrt{u}}$$

Z_i and Z_j are the ionic charges of the reactant species i and j, r_2 is the distance of closest approach between reactant species, and A and B are known constants with values of 0.509 $M^{-1/2}$ and 3.29 $M^{-1/2}$ nm^{-1}, respectively, in aqueous solution at 25 °C.[30]

The above function fits the data points well with $k_o = 3.59 \times 10^{-1}$ M^{-1} s^{-1}, $Z_iZ_j = 2.17$, and $r_2 = 9.8$ Å for k_{2s} (Figure 3), and $k_o = 5.69 \times 10^{-1}$ M^{-1} s^{-1}, $Z_iZ_j = 2.36$, and $r_2 = 8.9$ Å for k_{2f} (Figure 4). Since the charge of ESSE is −2, charges of −1.1 and −1.2 can be obtained from k_{2s} and k_{2f}, respectively, for 1-Cd_6MT-1. The calculated charges are significantly smaller than the net −3 charges of the M_3S_9 clusters. An alternative explanation, based on the NMR structure, is developed below.

Table 3. [PySSPy] Dependence of the Observed Rate Constants for the Reaction of Lobster Cd_6MT-1 and PySSPy

[PySSPy]/mM	$(k_s \pm \sigma) \times 10^3/s^{-1}$	$(k_f \pm \sigma) \times 10^2/s^{-1}$
0.3	1.37 ± 0.08	1.80 ± 0.08
0.4	1.77 ± 0.10	2.07 ± 0.04
0.6	2.54 ± 0.06	3.27 ± 0.10
0.8	3.19 ± 0.05	4.36 ± 0.07

[a] $[Cd]_{MT}$ = 5 μM; pH 7.4 in 5 mM Tris−HCl + 100 mM KCl at 25.0 °C.

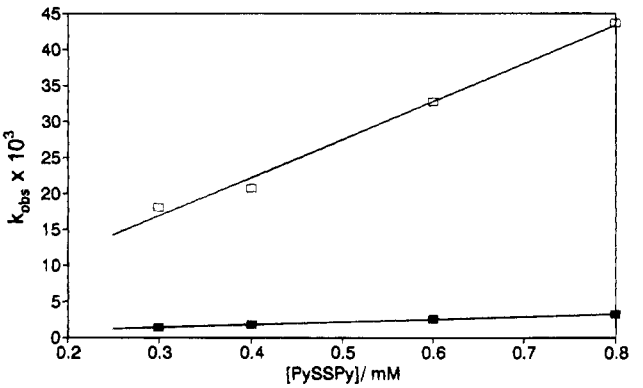

Figure 7. Plots of the observed rate constants vs [PySSPy] for the reaction of Cd_6MT-1 with PySSPy: k_s (■); k_f (□). Conditions are the same as in Figure 6.

Table 4. Ionic Strength Dependence of the Observed Rate Constants for the Reaction of Lobster Cd_6MT-1 with ESSE[a]

$\mu^{1/2}$	$k_{1s} \times 10^3/s^{-1}$	k_{2s}/M^{-1} s^{-1}	$k_{1f} \times 10^3/s^{-1}$	k_{2f}/M^{-1} s^{-1}
0.158	1.12	0.635	1.20	7.22
0.224	1.02	0.738	1.75	7.75
0.316	1.08	0.752	1.40	9.12
0.447	1.89	0.890	1.50	10.5
0.632	0.88	1.050	1.40	13.4

[a] $[Cd]_{MT}$ = 20 μM; pH 7.4 in 5 mM Tris−HCl at 25.0 °C.

Discussion

The reactions of ESSE, PySSPy, and related compounds with simple thiols and small peptides are rapid (typically on the stopped flow time scale), follow monophasic, second-order kinetics, and exhibit a strong influence of the charges of the thiol and disulfide on the magnitudes of the rate constants.[24,31,32] In the buffer system used in this study, the second-order rate constants for 50 μM glutathione (GSH) with excess ESSE (0.50 mM) and PySSPy (0.48 mM) were found to be 854 ± 2 and 3580 ± 250 M^{-1} s^{-1}, respectively (Schultz, J. Unpublished observation). They are about 2−3 orders of magnitude larger than the second-order constants for the corresponding MT reactions. Thus, the slower kinetics and four-term rate laws for MT (eqs 1 and 4, Table 5) can be correctly ascribed to the interactions of the two disulfides (ESSE and PySSPy) with the two-domain structure of metallothionein rather than the intrinsic reactivity of the disulfides.

2-D NMR studies have established the metal-thiolate connectivities of lobster MT-1 (Figure 8).[22,23] Each cluster is created within a distinct domain: cysteine residues 5 through 27 form the β_N-domain cluster and cysteines 30 through 56 form the β_C-domain cluster. Both are three-metal type-B clusters, while the mammalian α- and β-domains contain four- and three-metal (or A- and B-type) clusters. There are additional important differences in structure between the mammalian and

(28) Brouwer, M.; Hoexum-Brouwer, T.; Cashon, R. E. *Biochem. J.* **1993**, *294*, 219−225.
(29) Snyer, G. H.; Cennerazzo, M. J.; Karalis, A. J.; Field, D. *Biochemistry* **1981**, *20*, 6509−6519.
(30) Nolte, H. J.; Rosenberry, T. L.; Neumann, E. *Biochemistry* **1980**, *19*, 3705−3711.
(31) Snyder, G. H.; Cennerazzo, M. J.; Karalis, A. J.; Field, D. *Biochemistry* **1981**, *20*, 6509−6519.
(32) Legler, G. *Biochim. Biophys. Acta* **1975**, *405*, 136−143.

Table 5. Rate Constants for the Reactions of Lobster and Rabbit Liver MTs with ESSE and PySSPy

reactants	slow step components $k_{1s} \times 10^3/s^{-1}$	slow step components $k_{2s}/M^{-1}\,s^{-1}$	fast step components $k_{1f} \times 10^3/s^{-1}$	fast step components $k_{2f}/M^{-1}\,s^{-1}$	ref
PySSPy *lob*-Cd_6MT1	0.30	3.65	1.00	52.9	*a*
PySSPy *lob*-Cd_6MT2	0.68	5.71	1.65	104.5	*a*
ESSE *lob*-Cd_6MT1	1.01	0.702	4.77	5.80	*a*
ESSE *lob*-Cd_6MT2	1.23	0.66	2.27	8.13	16
ESSE *rab*-Cd_7MT2	0.42	0.12	1.26	1.75	17
ESSE *rab*-α-domain	nd[c]	nd	0.64	1.12	14
ESSE *rab*-β-domain	0.14	0.062	nd	nd	*b*

[a] This work. [b] Munoz, A.; Petering, D. H.; Shaw, C. F., III. Unpublished results. [c] nd = not detected.

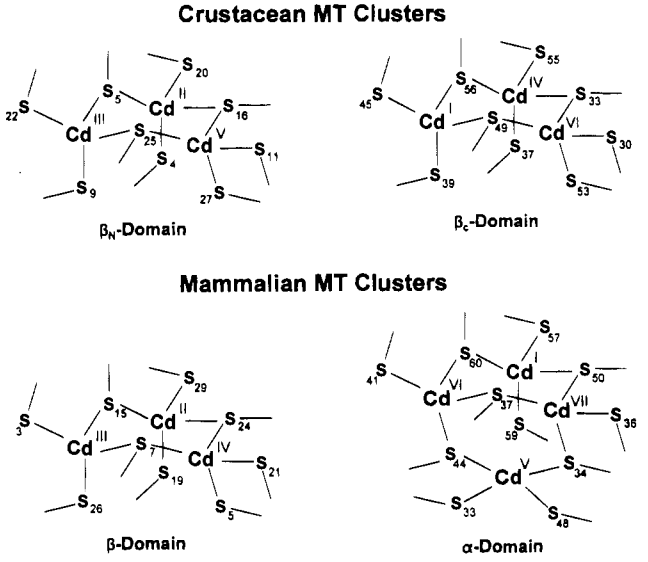

Figure 8. Cluster structures for lobster[22,23] and mammalian[6-9] MTs.

lobster proteins. A number of the thiolates assigned as homologous in the sequence comparison[19] are bridging in one structure and terminal in the other: for example, *lob*-cys-11 vs *mam*-cys-15 and *lob*-cys-45 vs *mam*-cys-50.[23] Only Cd II of the lobster protein has an exact structural homologue, Cd IV, in the mammalian protein. The remaining Cd ions typically have only two thiolates in common with the similar Cd ions of the mammalian structure.[22,23] These differences are reflected in the dissimilarities of the circular dichroism spectra of mammalian and crustacean (*Scylla serrata*) MTs,[33] and as discussed below also give rise to altered chemical reactivity of the lobster protein.

The biphasic kinetics of the reactions of lobster Cd_6-MT-1 with ESSE and Cd_6-MT-1 and -2 with PySSPy demonstrate that the reaction of Cd_6MT-2 and ESSE reported previously[16] is not unique. Indeed each MT isoform reacts biphasically with each of the two electrophiles. Since MTs of two different stoichiometries (two M_3S_9 clusters in crustacean MTs, vs M_3S_9 and M_4S_{11} clusters in mammalian MTs) exhibit biphasic kinetics, it is likely that this property reflects a fundamental characteristic related to the biological functions of these enigmatic proteins. MTs are induced by a diverse array of biological conditions,[1-5] and the possibility that each domain (cluster) has a unique function has been proposed. The systematic differences in domain reactivity reflected in the biphasic reactions are consistent with this proposal.

In contrast to the four-term rate law (eqs 1 and 4) for reactions of lobster MT-1 & -2 with PySSPy and ESSE and for mammalian MT reactions with ESSE (Table 5), the very slow reaction of rabbit liver MT with oxidized glutathione (GSSG, which bears a net −2 charge)[17,18] is a single second-order process (rate = k_2[MT][GSSG]; k_2 = 0.005 $M^{-1}\,s^{-1}$).[18] The rate constant is 10^2−10^4 times slower than second order terms for ESSE reactions with mammalian and lobster MTs. Disulfide interchange reactions with GSSG lack the strong driving force provided by the easily reduced disulfide bonds of PySSPy and ESSE. A monophasic reaction, as observed by Maret,[18] would be expected if (1) GSSG is more reactive toward the α-cluster than the β-cluster, as are ESSE,[14] aurothiomalate (Munoz, A.; Shaw, C. F., III. Unpublished results), Melphalan,[34] and nitrilotriacetic acid,[35] and (2) the β-domain reacts with the partially or fully oxidized α-domain more rapidly than with GSSG. Because both phases of the ESSE and PySSPy reactions are much faster than the GSSG reaction, their independent reactions with each domain are observable, as found here and previously.[12,14,16]

Kinetic comparisons of the aromatic disulfides PySSPy and ESSE, which bear charges of 0 and −2, respectively, effectively probe the role of electrostatics on the reactions of MT thiolates. PySSPy, like ESSE, reacts stoichiometrically with MT thiolates and the reaction kinetics are easily monitored. The observed rate constants obtained with similar concentrations of disulfide reagent are consistently larger for PySSPy. For Cd_6MT-2 and 0.5 mM RSSR, the observed rate constants, k_s and k_f, are 3.72 × 10^{-3} s^{-1} and 5.38 × 10^{-2} s^{-1}, respectively, for PySSPy (Table 2), and 1.35 × 10^{-3} s^{-1} and 0.38 × 10^{-2} s^{-1} for ESSE.[16] Since crustacean MTs are negatively charged, the slower reactions of ESSE suggest that there is a significant electrostatic influence on the rates. This effect is clearly reflected in the second-order rate constants which describe bimolecular interactions of the disulfides with MT: k_{2f} values for PySSPy are about 10 times greater than for the corresponding ESSE reaction with the same isoprotein (Table 5); the k_{2s} values similarly vary by a factor of five.

The positive salt effect for ESSE (Table 4, Figures 3 and 4) confirms the role of electrostatic repulsions on the rate of its reaction with Cd_6-MT-1 and is consistent with earlier model compound studies.[29] The quantitative Debye−Hückel treatment of ionic strength effects on k_{2s} and k_{2f} yields charges of −1.1 and −1.2, respectively, for the two reactive centers of the protein. These values, based on the assumption inherent in the Debye−Hückel relationship that the charges on MT are centrally located, are in excellent agreement with the net charges (−1) of the β_C and β_N domains calculated from NMR domain structures[23] and the amino acid sequence.[19] They are much smaller than the net −3 charges of the M_3S_9 clusters. In detailed studies of electron transfer reactions, overall protein charge, not the local charge at the site(s) of protein-ligand interaction, determine the electrostatic effects.[36,37] On that basis the effective charges of *ca.* −1 determined from the Debye−Hückel treatment of the rates can be associated with the two protein domains.

The biphasic kinetics and the excellent agreement between the domain charges from the primary and tertiary structure and

(33) Law, A. Y-C.; Cherian, M. G.; Stillman, M. J. S. *Biochim. Biophys. Acta* **1984**, *784*, 53−61.
(34) Yu, X.; Wu, S.; Fenselau, C. *Biochemistry* **1995**, *34*, 3378−3385.
(35) Otvos, J. D.; Liu, X.; Li, H.; Shen, G.; Basti, M. In *Metallothionein III*; Suzuki, K. T., Imura, N., Kimura, M., Eds.; Springer Verlag: Basel, 1993; pp 57−74.
(36) Feinberg, B. A.; Ryan, M. D. *Top. Bioelectrochem. Bioenerg.* **1981**, *4*, 225−269.
(37) Feinberg, B. A.; Ryan, M. D.; Wei, J.-F. *Biochem. Biophys. Res. Commun.* **1977**, *79*, 769−775.

from the Debye–Hückel treatment are consistent with independent reactions of the two lobster MT domains. For mammalian MTs independent reactions of the domains have been conclusively demonstrated in the reactions of ESSE with rabbit MT α-domain[14] and β-domain (Muñoz, A. Unpublished results); and rabbit MT with aurothiomalate (Muñoz, A. Unpublished results), EDTA,[38] and NTA-MT.[35]

Since each domain of lobster Cd_6MT-1 has a net charge of −1, the differential reactivities of the domains arise from effects more subtle than the net domain charges. Unlike electron transfer reactions where bond making and bond breaking are unimportant,[36] the DTNB-MT reaction proceeds through intermediates in which mixed disulfides, MT-SSE, with thionitrobenzoate (ES^-) are formed and react further.[12,17] The metal–thiolate connectivities shown in Figure 8[22,23] reveal pronounced differences in the protein folding between the β_C and β_N domains. These structural differences, particularly the local environments around the solvent-accessible thiolate ligand atoms, govern the energetics of the bond making and bond breaking and can, therefore, distinguish the two clusters kinetically, leading to the observed fast and slow steps, despite the similarity of the electrostatic contributions for each cluster.

The first-order rate constants for the lobster MT reactions with PySSPy and ESSE (Table 5) lie within a small ranges of values: $(0.3-1.2) \times 10^{-3}$ s^{-1} for the slow step and $(1.0-4.8) \times 10^{-3}$ for the fast step. Similar first-order constants are found for a variety of mammalian MT reactions with electrophiles,[10,12,14] metal-chelating ligands,[35,39] and aurothiomalate[13] and for MT metal exchange.[40] The activation enthalpies for the *lob*-MT-2–ESSE first-order reaction components are large and negative,[16] −185 and −194 J/(mol s) for k_{1s} and k_{1f}, respectively, suggesting that during the rate-determining step a substantial rearrangement precedes the reaction of the metal-bound thiolate with ESSE.[16] This process, which is rate limiting for a vast variety of reactants with MTs from two distinct phyla, may reflect a fundamental motion or conformational change of the protein.

Differences in the metal–thiolate connectivities which distinguish the lobster β_C and β_N clusters from one another and from the mammalian β-cluster were revealed by the 2-D NMR structure.[22,23] Lack of lobster MT cross-reactivity to antimammalian MT antibodies (Abel, J.; deRuiters, N.; Shaw, C. F., III; Schultz, J. Unpublished data) and differences in the circular dichroism spectra between the homologous crab MT and mammalian MT[33] are consistent with these differences. The unique thiolate connectivities imply an altered tertiary structure which, in turn, generates modified chemical reactivity in the lobster MTs. Table 5 shows the lobster MT-1 and -2, are kinetically more reactive than their mammalian counterparts. The fast- and slow-phase second-order rate constants for the lobster protein reaction with ESSE are greater than the corresponding rabbit MT rate constants. These structural and kinetic differences may reflect altered function, for example the role of MT as a copper donor during the molt cycle of the crustacean.[28,41] The lobster model continues to provide useful comparisons of the structures, reactivity and biological functions between two distinct phyla. The finding that the crustacean β-clusters with altered tertiary structures exhibit enhanced thiolate reactivity, shown here by their accelerated reactions with ESSE, is particularly noteworthy.

Acknowledgment. This research was supported by the U.S. NIH (Grants ES-04026 and ES-04184). We thank Dr. Meral Savas, Dr. Amalia Muñoz, and Mr. Joseph Schultz for helpful discussions and Mr. Chris Kosteretz for his skilled husbandry of the lobsters. C.F.S. thanks the U.S. NIH for a Senior Fellowship and the Deutsches Forschungsgemeinschaft for a Gastprofessorship and the Medizinisches Institut für Umwelthygiene, Düsseldorf, Germany, for its hospitality during 1993–1994 when the manuscript was completed.

IC950266K

(38) Gan, T.; Muñoz, A.; Shaw, C. F., III; Petering, D. H. *J. Biol. Chem.* **1995**, *270*, 5339–5345.
(39) Li, Ti-Y.; Kraker, A. J.; Shaw, C. F., III; Petering, D. H. *Proc. Natl. Acad. Sci. U.S.A.* **1980**, *77*, 6334–6338.
(40) Kägi, J. H. R. In *Metallothionein III*; Suzuki, K. T., Imura, N., Kimura, M., Eds.; Springer Verlag: Basel, 1993; pp 29–56.
(41) Brouwer, M.; Whaling, P.; Engel, D. W. *Environ. Health Perspect.* **1986**, *65*, 93–100.